HONEST 3 The high end of Pulsar spectra

HOT TOPICS IN HIGH ENERGY ASTROPHYSICS

Prospects for the detection of very-high-energy pulsars with LHAASO and SWGO

KAI-KAI DUAN (PURPLE MOUNTAIN OBSERVATORY)
WORK WITH QUAN HU, YI ZHANG, HOU-DUN ZENG

2024-11-28 @3RD HONEST WORKSHOP

https://doi.org/10.1093/mnras/stae1497

Outline

- Observations of VHE pulsars
- Method for sensitivity of the pulse signal
- Results and summary

Four VHE pulsars detected by IACTs

Name	RA	Dec	Type	Discoverer	Date
			...	...	
Crab Pulsar	05 34 31.9	+22 00 52.2	PSR	MAGIC	2008.11
Vela Pulsar	08 35 20.7	-45 10 35.2	PSR	H.E.S.S.	2014.06
Geminga Pulsar	06 33 54.153	+17 46 12.91	PSR	MAGIC	2018.06
PSR B1706-44	17 09 42.62	-44 29 05.8	PSR	H.E.S.S.	2019.07

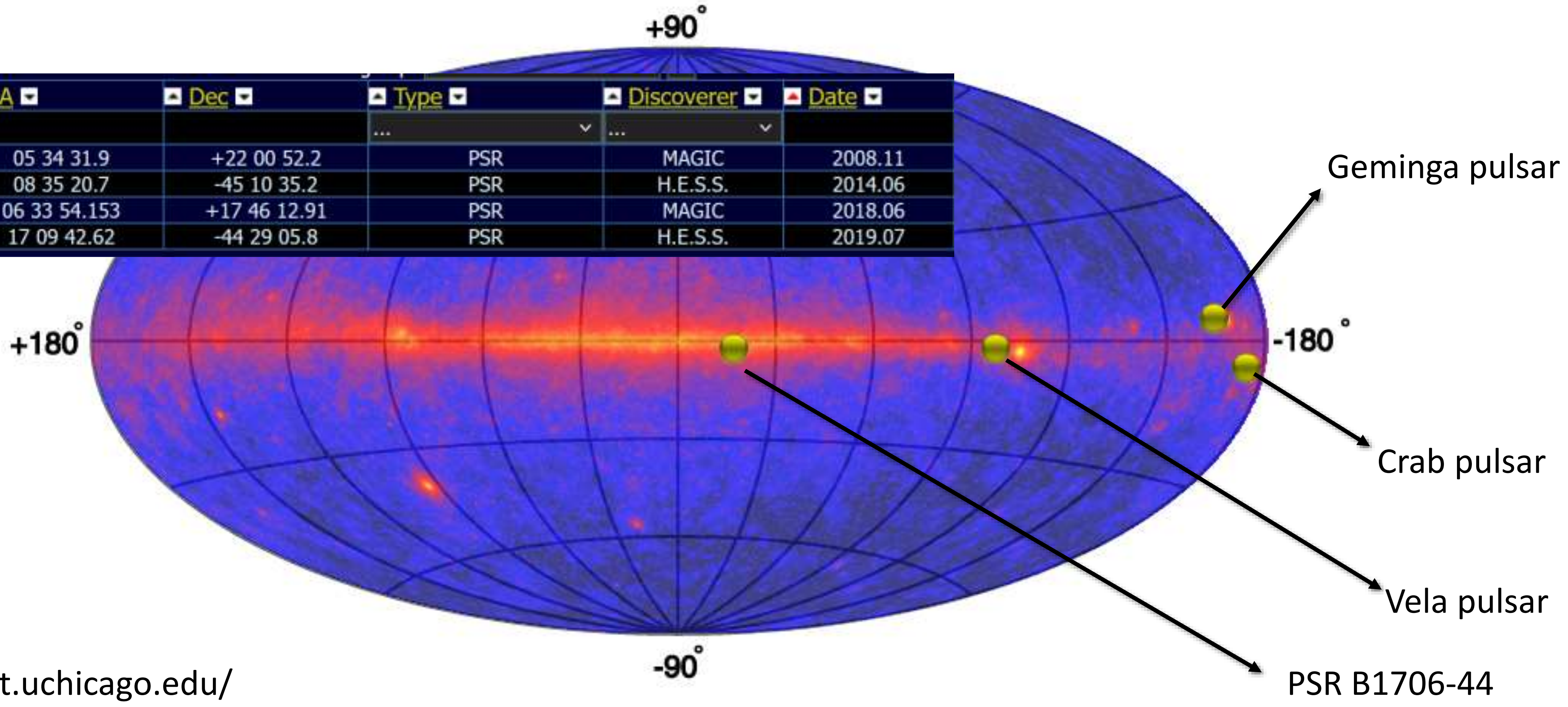

Credit: http://tevcat.uchicago.edu/

Observation of the Pulsed γ-Rays of Crab pulsar
(Teraelectronvolt pulsed emission from the Crab Pulsar detected by MAGIC)

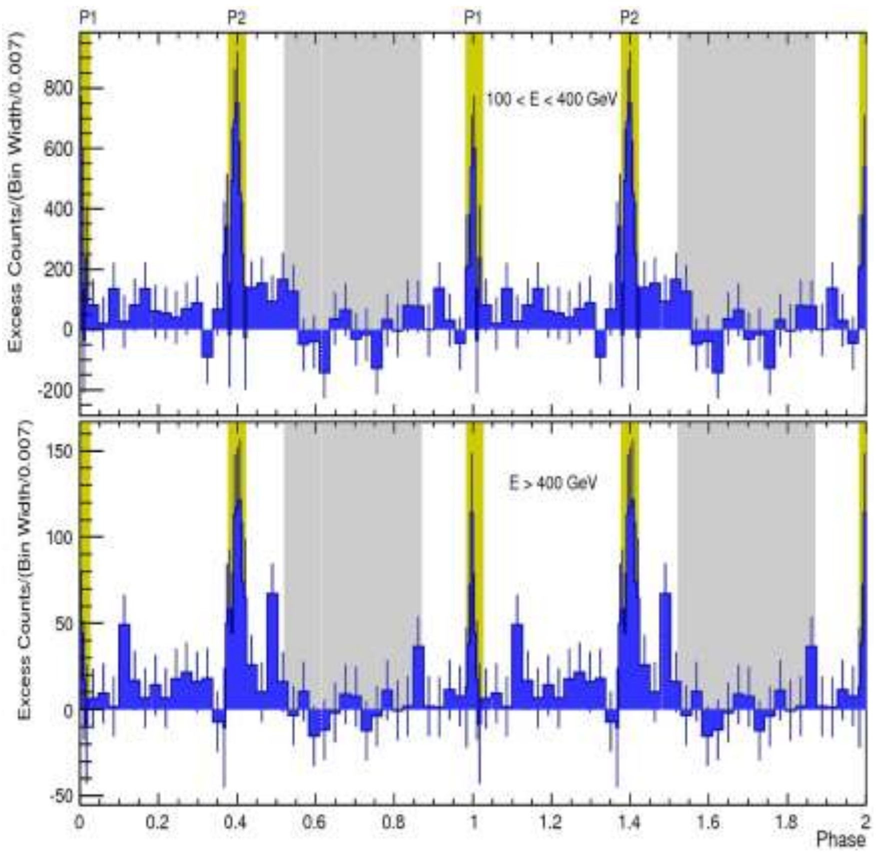

pulse profile

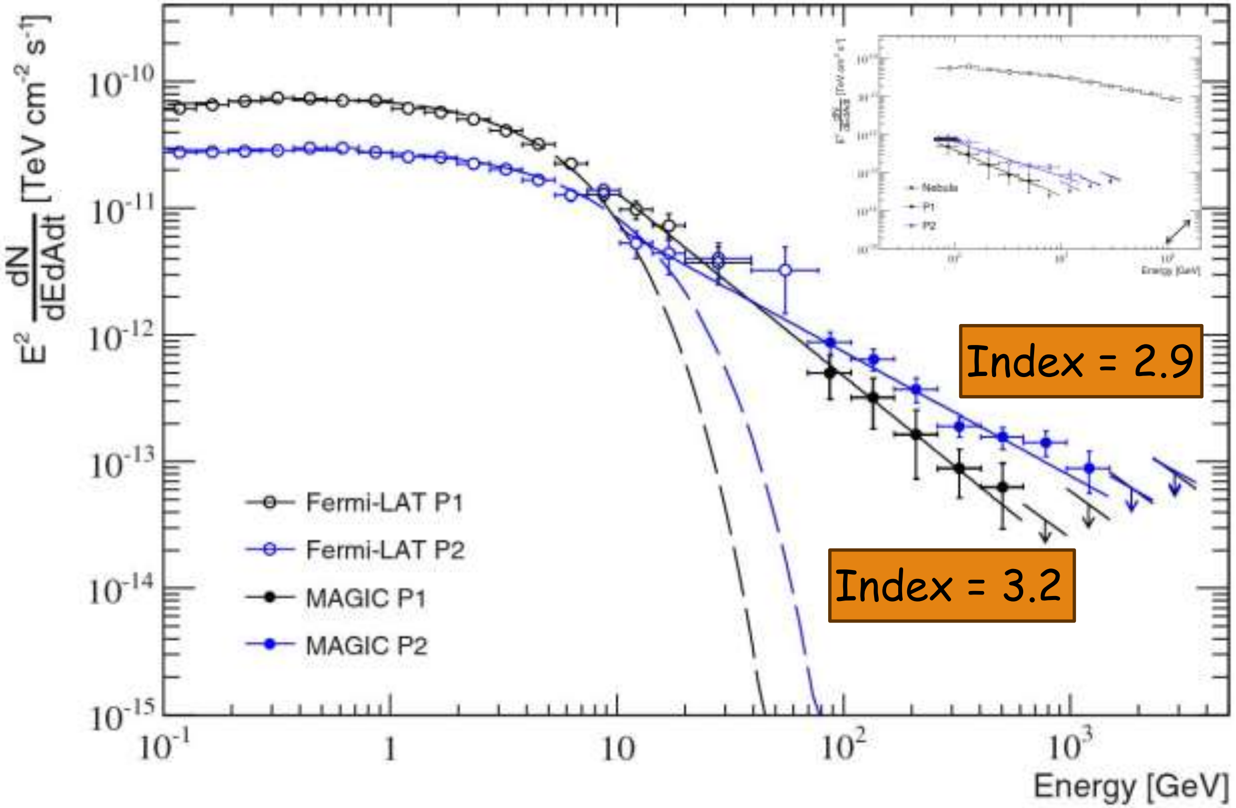

SED

MAGIC Coll. A&A, 585 (2016) A133

Observation of the Pulsed γ-Rays of Vela pulsar

(Discovery of a radiation component from the Vela pulsar reaching 20 teraelectronvolts)

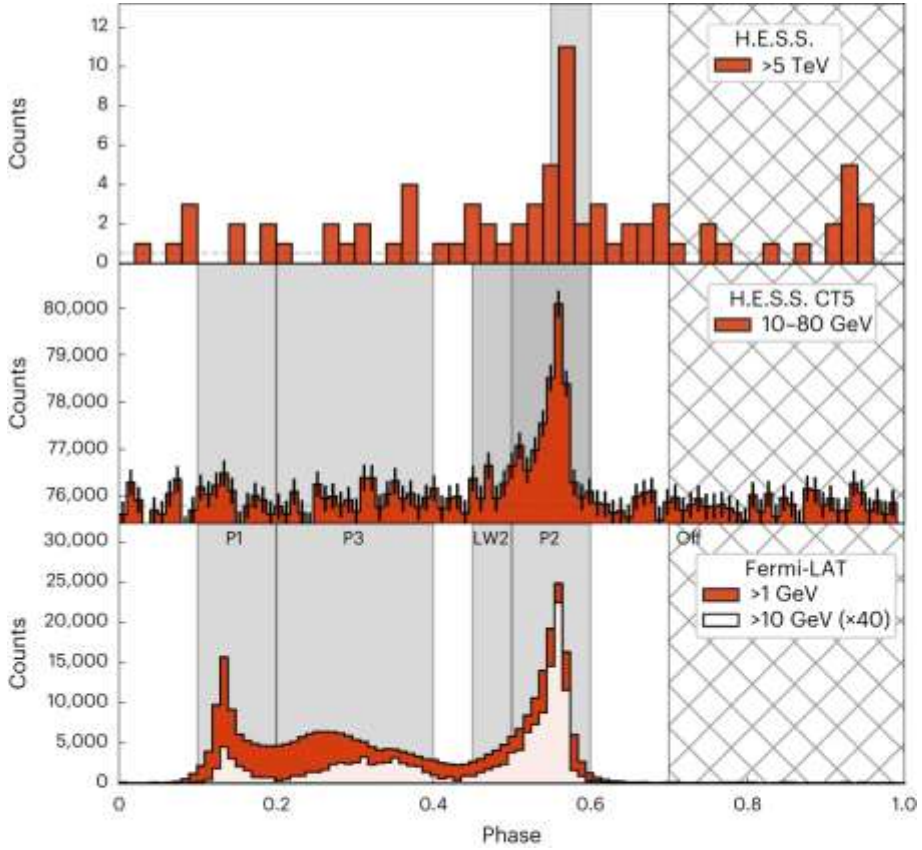

pulse profile

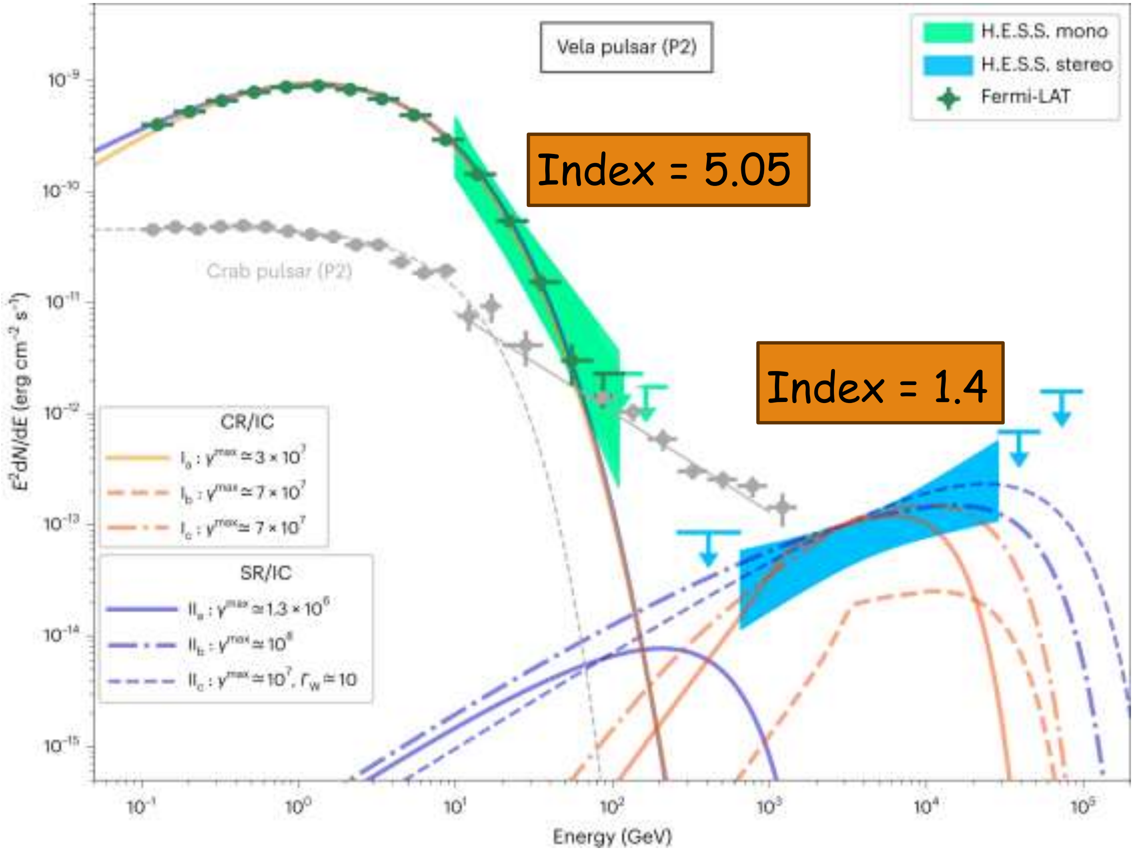

SED [HESS Coll. Nat Astron **7**, 1341–1350 (2023)](#)

Observation of the Pulsed γ-Rays of Geminga pulsar and PSR B1706-44

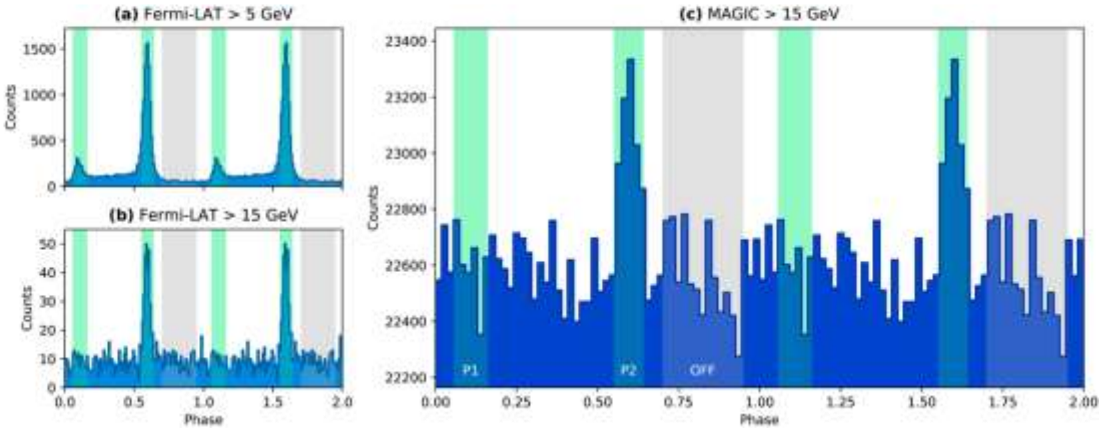

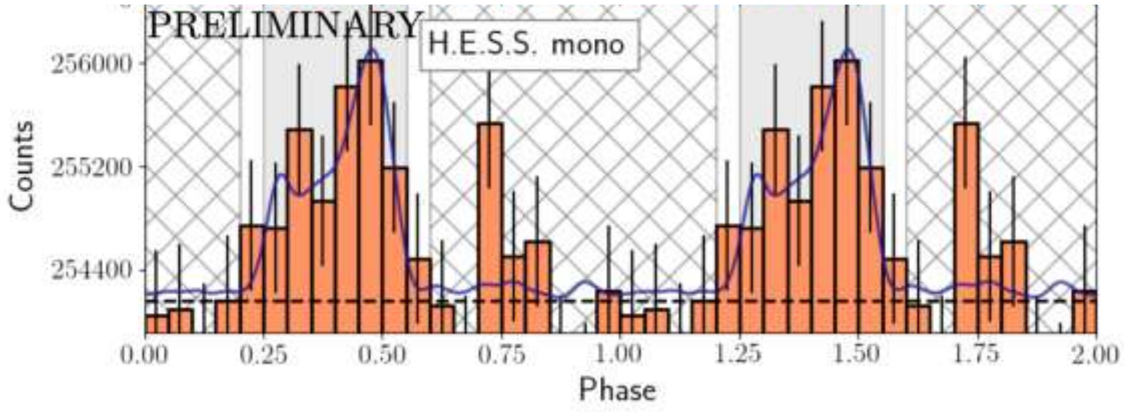

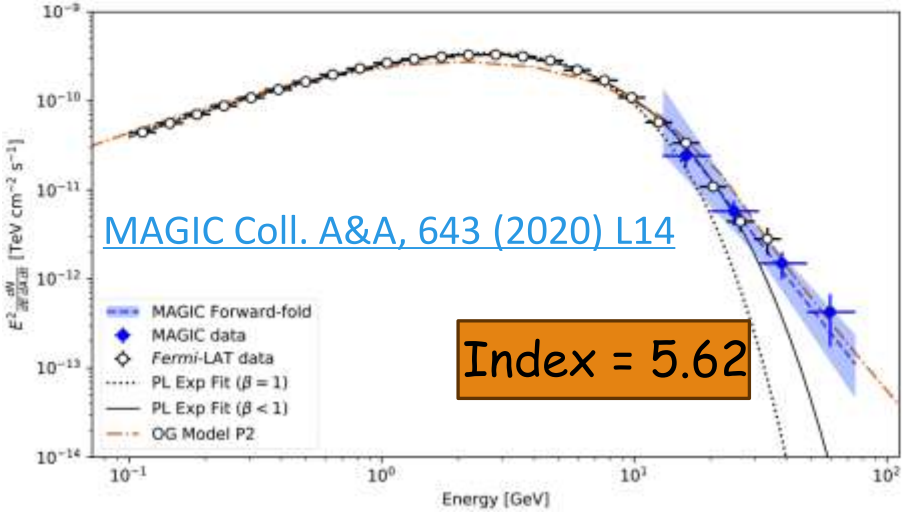

MAGIC Coll. A&A, 643 (2020) L14

Index = 5.62

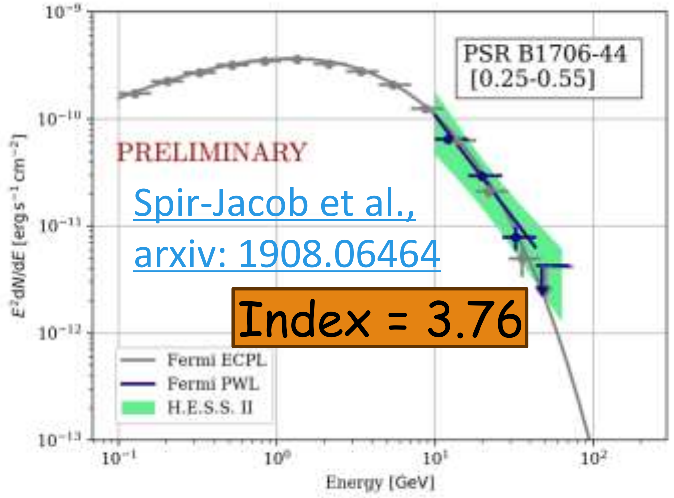

Spir-Jacob et al., arxiv: 1908.06464

Index = 3.76

Sketch of the pulsar's magnetosphere, particle acceleration and gamma-ray emission

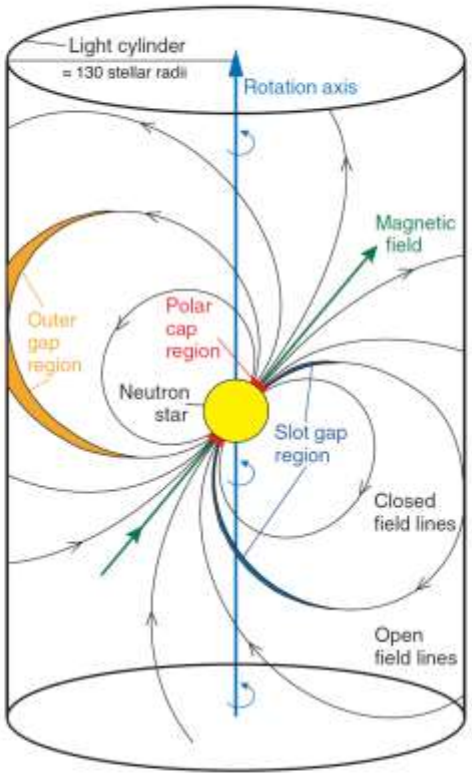

Fig. 1. A sketch of the Crab pulsar's magnetosphere. Electrons are trapped and accelerated along the magnetic field lines of the pulsar and emit electromagnetic radiation via the synchrotron-curvature mechanism. Vacuum gaps or vacuum regions occur at the polar cap (*1–3*) very close to the neutron star surface in a thin layer extending for several stellar radii along the boundary of the closed magnetosphere, the so-called slot gap (*4–6*), and in the outer region (*7–9*) close to the light cylinder (the outer gap). Vacuum gaps are filled with plasma, but its density is lower than the critical Goldreich-Julian density (*24*), in which the magnetically induced electric field is saturated, and therefore electrons can be accelerated to very high energies. Absorption of high-energy γ-rays occurs by interaction with the magnetic field (magnetic pair production) as well as with the photon field (photon-photon pair production). The former dominates close to the surface of the neutron star where the magnetic field is strongest; it leads to a superexponential cutoff at relatively low energies (few giga–electron volts). Photon-photon collisions prevail farther out in the magnetosphere close to the light cylinder, where the magnetic field is lower, and lead to a roughly exponential cutoff at higher (>10 GeV) energies.

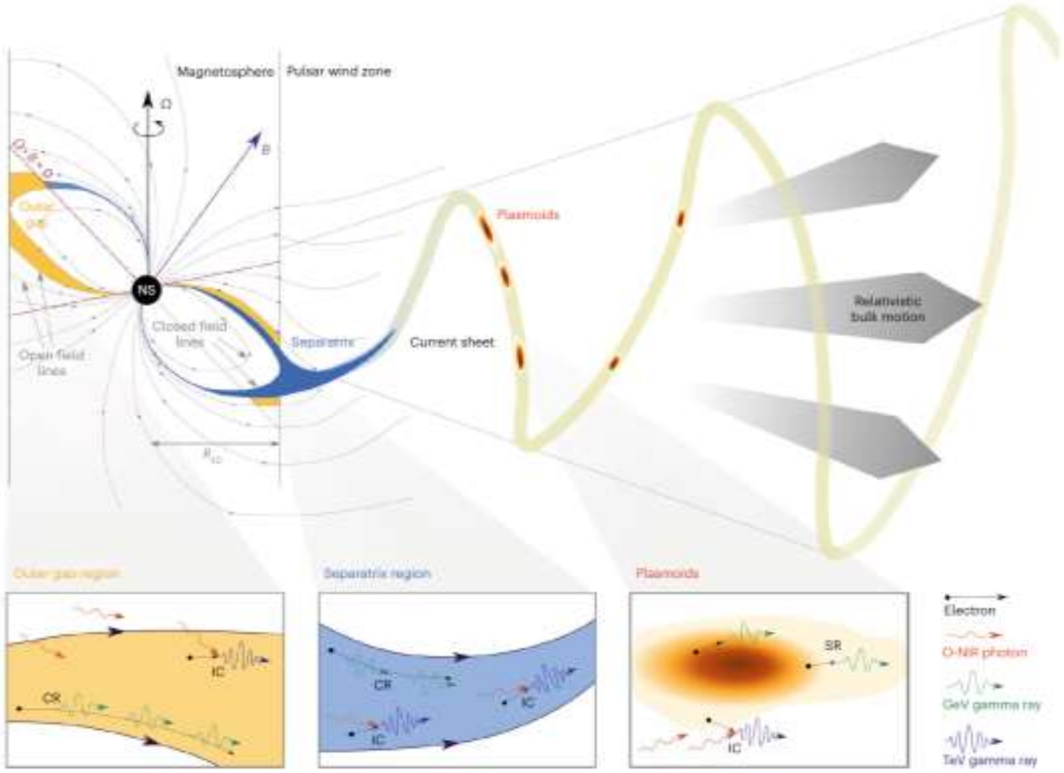

MAGIC Coll. DOI: 10.1126/science.1164718

HESS Coll. DOI: 10.1038/s41550-023-02052-3

Outline

- Observations of VHE pulsars
- Method for sensitivity of the pulse signal
- Results and summary

Field of view of LHAASO and SWGO

LHAASO
Latitude : 30° N
FoV: ~50 °

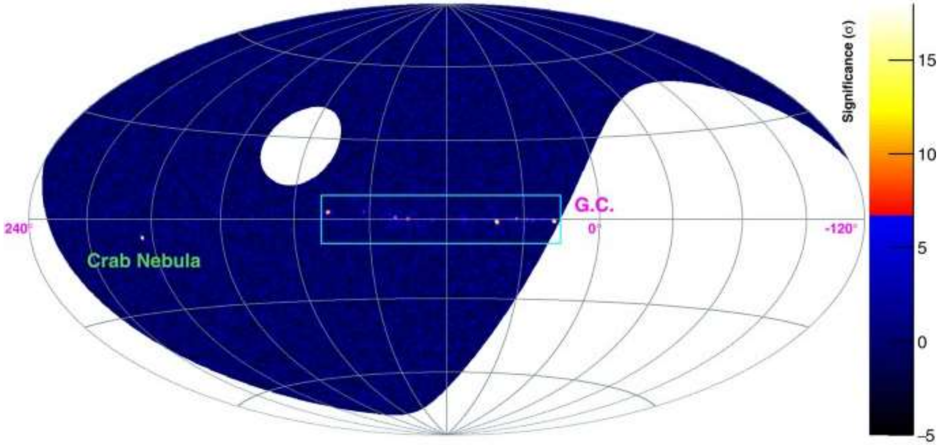

Crab pulsar,

Geminga pulsar

in FoV of LHAASO

Credit : https://ihep.cas.cn/lhaaso/

SWGO
Latitude : 23° S
FoV: ~60 °

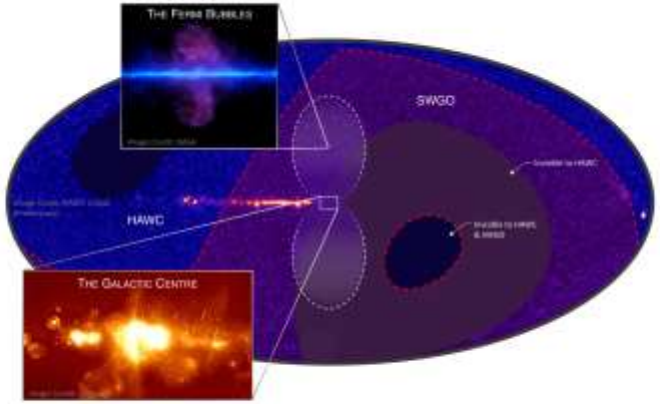

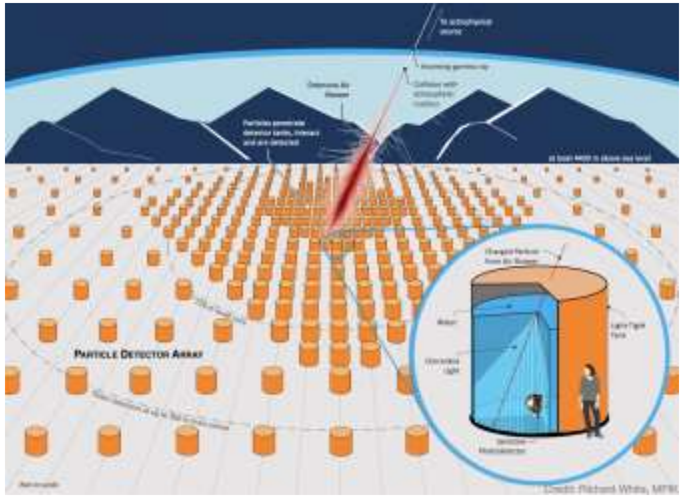

Vela pulsar,

PSR B1706-44

in FoV of SWGO

Credit : https://www.swgo.org/

Sensitivity of LHAASO and SWGO for point source

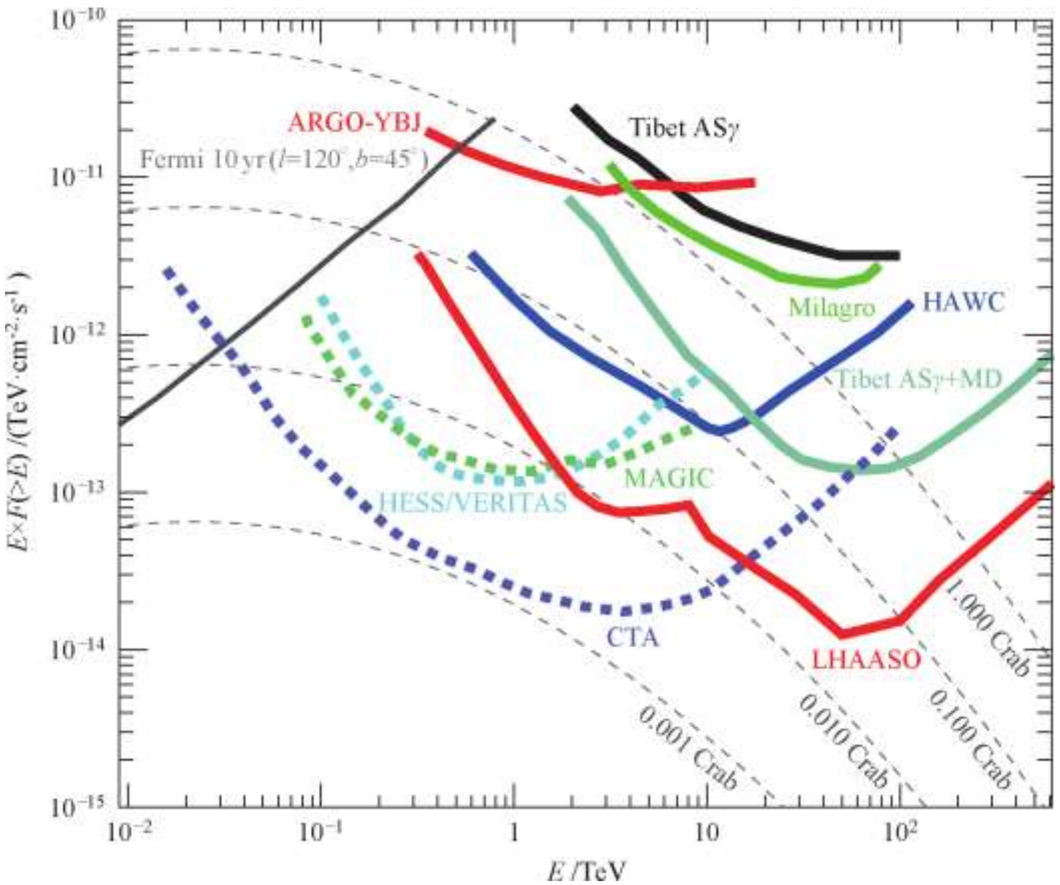

LHAASO Coll. DOI: 10.1016/j.chinastron.2019.11.001

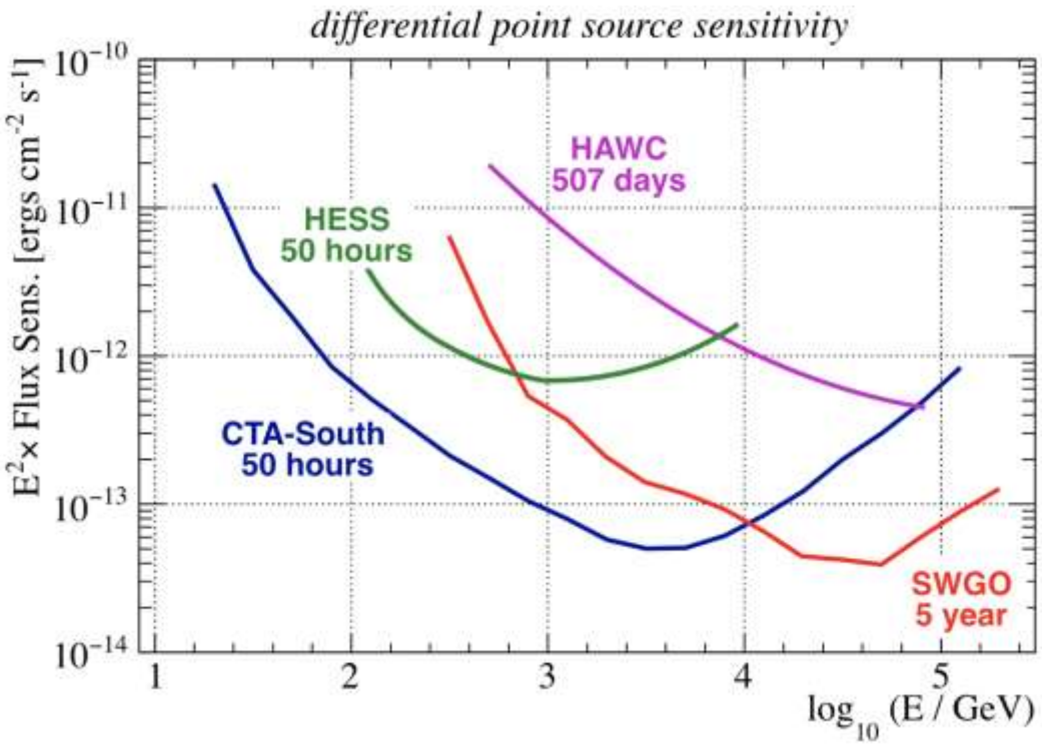

SWGO Coll. arxiv: 1907.07737

Method for sensitivity of the pulse signal

point source sensitivity:

$$S = \frac{N_s}{\sqrt{N_{cr}}}$$

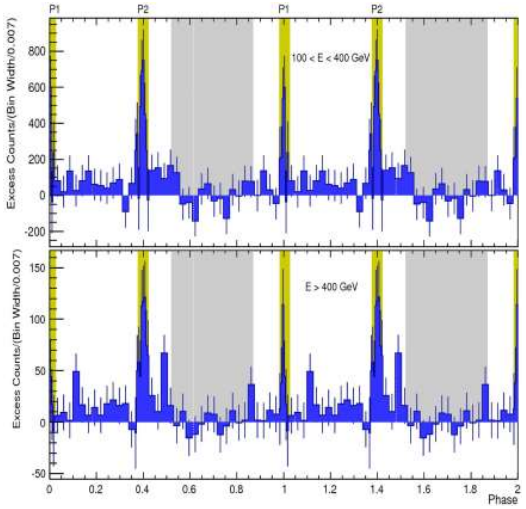

pulse signal sensitivity:

$$S = \frac{N_p^{\mathrm{onP}}}{\sqrt{N_{\mathrm{cr}}^{\mathrm{onP}} + N_{\mathrm{nebula}}^{\mathrm{onP}}}} = \frac{N_p^{\mathrm{onP}}}{\sqrt{(1+\beta) N_{\mathrm{cr}}^{\mathrm{onP}}}}$$

N_p^{onP}: The number of pulse signal events in the on-pulse region

$N_{\mathrm{cr}}^{\mathrm{onP}}$: Cosmic ray background events in the on-pulse region of pulsar

$N_{\mathrm{nebula}}^{\mathrm{onP}}$: Gamma-ray events from nebula in the on-pulse region of pulsar

$$N_{\mathrm{cr}}^{\mathrm{onP}} = \alpha N_{\mathrm{cr}}$$

$$\beta = \frac{N_{\mathrm{nebula}}}{N_{\mathrm{cr}}} = \frac{F_{\mathrm{nebula}} r_\gamma f_{\mathrm{ROI}}}{F_{\mathrm{cr}} r_{\mathrm{cr}} \Delta\Omega}$$

Cosmic ray background

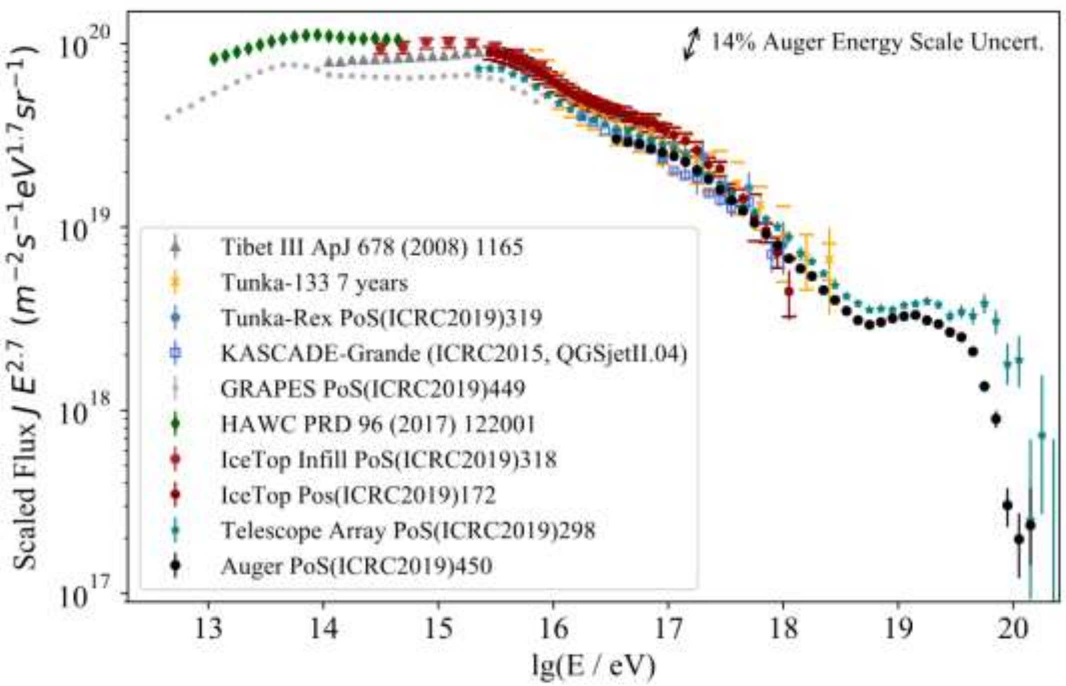

Spectrum of the high-energy cosmic rays

(from ICRC 2019 -- Cosmic Ray Indirect Rapport)

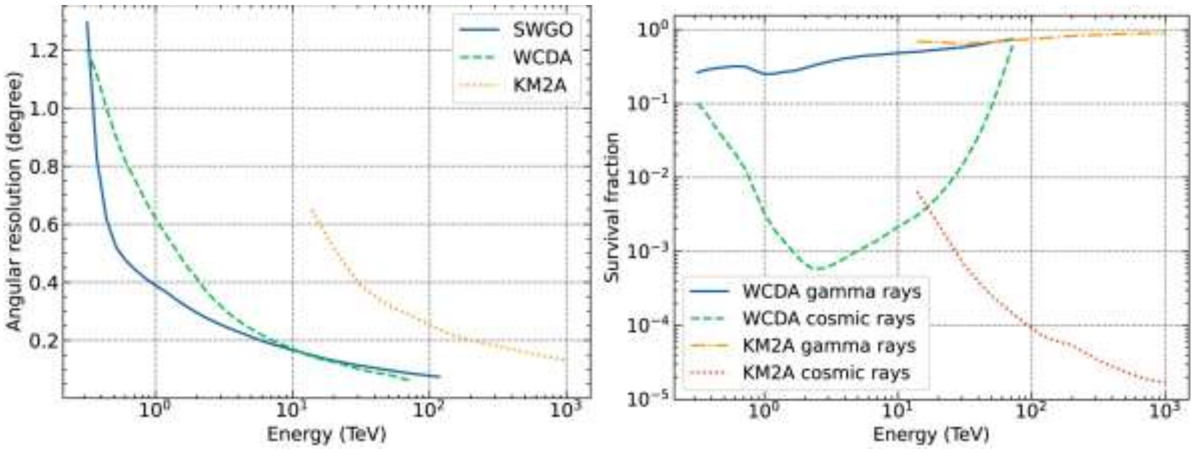

Angular resolution and survival fraction of LHAASO and SWGO

$$N_{cr} = F_{cr} r_{cr} \Delta\Omega$$

$$N_{\mathrm{cr}}^{\mathrm{onP}} = \alpha N_{\mathrm{cr}}$$

Extension and spectrum of crab nebula

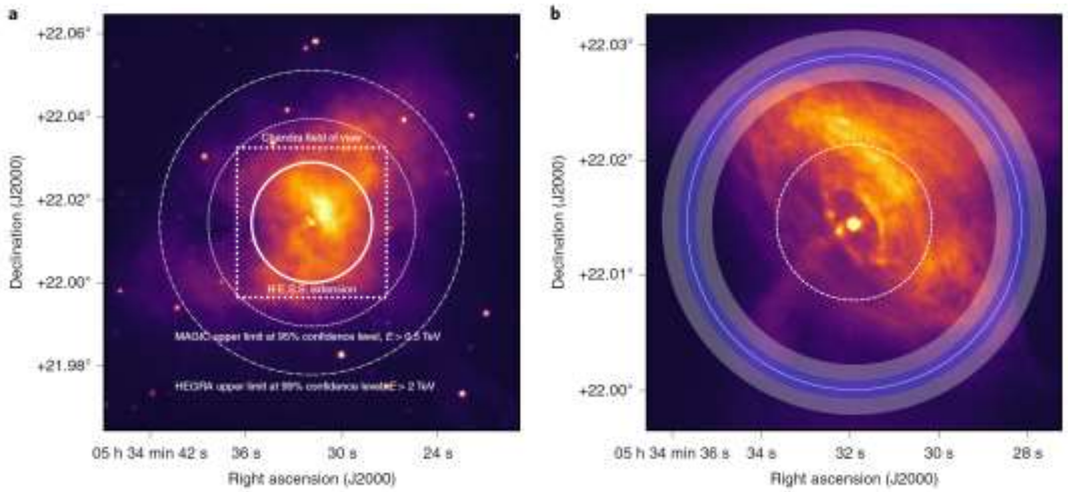

Fig. 1 | Images of the Crab nebula. a, Ultraviolet (wavelength $\lambda = 291$ nm) image recorded with the Optical-UV Monitor onboard XMM-Newton[30] (filter UVW1). The MAGIC and HEGRA extension upper limits of 2.2′[10] and 1.5′[14] are drawn as dash-dotted and dashed lines, respectively. The extent of the sky region shown in **b** is indicated as a dotted square, and the High Energy Stereoscopic System (H.E.S.S.) extension (two-dimensional Gaussian σ corresponding to 39% of the measured events) is drawn as a solid circle. All circles are centred on the Crab pulsar position for illustration purposes; in the fitting procedure determining the H.E.S.S. extension described in the main text the centroid position is left free. **b**, Chandra X-ray image[11] (courtesy of M. C. Weisskopf and J. J. Kolodziejczak). The H.E.S.S. extension is shown as a solid white circle overlaid on top of shaded annuli indicating the statistical and systematic uncertainties of our measurement. The Chandra extension, corresponding to 39% of the X-ray photons, is drawn as a dashed white circle.

HESS Coll. DOI: 10.1038/s41550-019-0910-0

Extension = 52 arcseconds

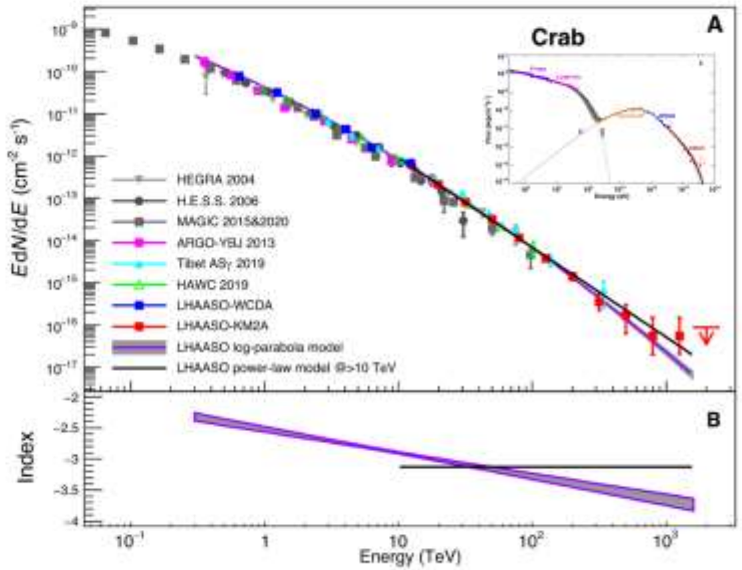

LHAASO Coll. DOI: 10.1126/science.abg5137

log-parabola spectrum

$$dN/dE = (8.2 \pm 0.2) \times 10^{-14} (E/10\ \text{TeV})^{-\Gamma}\ \ \text{cm}^{-2}\ \text{s}^{-1}\ \text{TeV}^{-1}$$

$$\Gamma = (2.90 \pm 0.01) + (0.19 \pm 0.02) \log_{10}(E/10\ \text{TeV})$$

Extension and spectrum of Vela X nebula

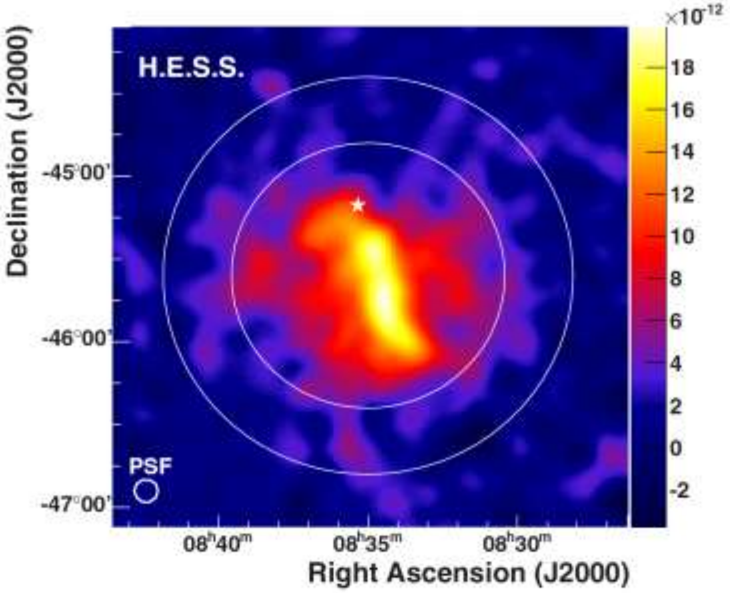

Fig. 4. H.E.S.S. VHE γ-ray surface brightness (cm^{-2} s^{-1} deg^{-2}) of Vela X integrated between 0.75 TeV and 70 TeV and 0.07° Gaussian smoothing width. The 0.07° PSF achieved with the X_{eff} method applied in this analysis is also shown for comparison. The circles are drawn with radii of 0.8° and 1.2°, respectively, around the central position of the VHE γ-ray emission. The white star marks the position of the pulsar PSR B0833-45.

Extension = 0.51 degree

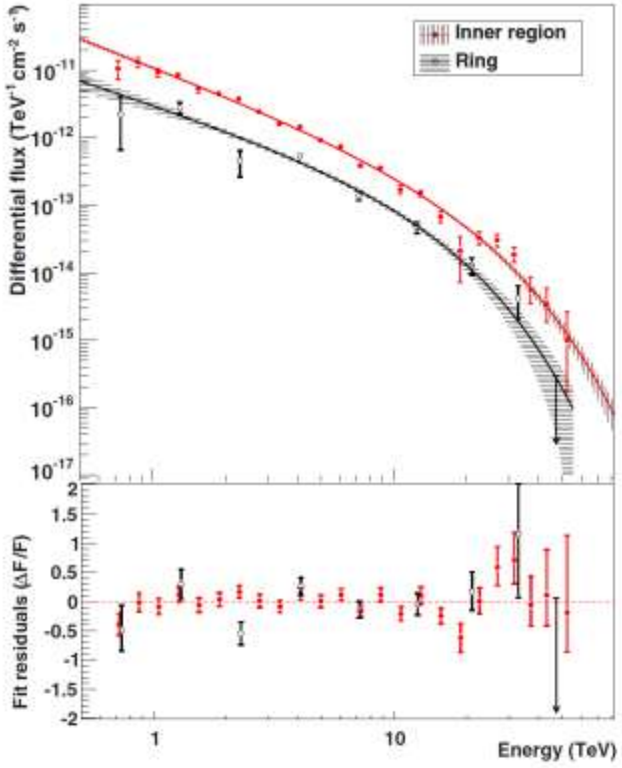

Fig. 2. Differential γ-ray spectrum of Vela X in the TeV energy range. Filled red circles: inner integration region <0.8°; open black circles: ring extension (between 0.8° and 1.2°). Both spectra are fitted with a power law with exponential cutoff. The shaded bands correspond to the statistical uncertainty of the fit.

Power-law with cutoff spectrum
Index = 1.36
Ecut = 13.9 TeV

HESS Coll. DOI: 10.1051/0004-6361/201219919

Extension and spectrum of Geminga

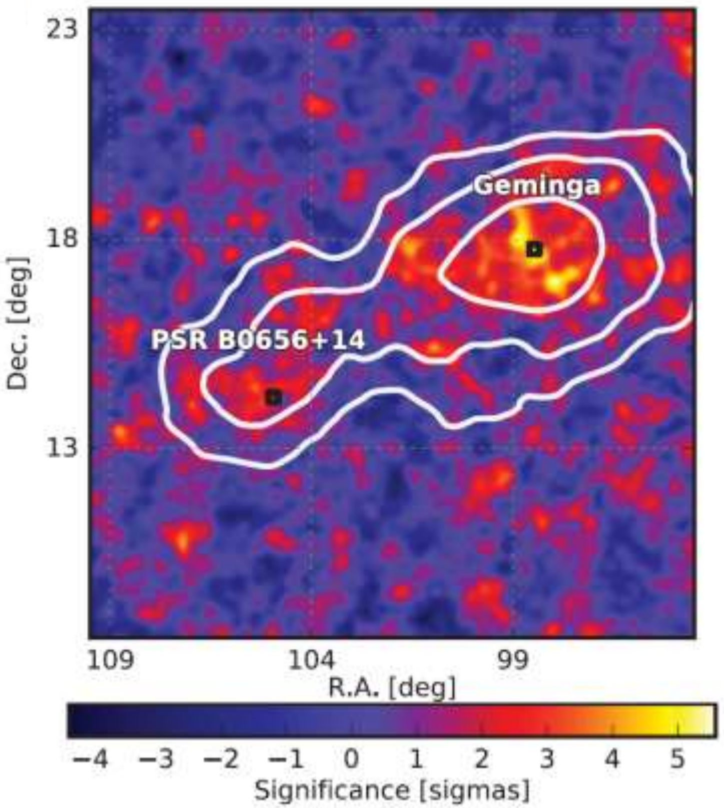

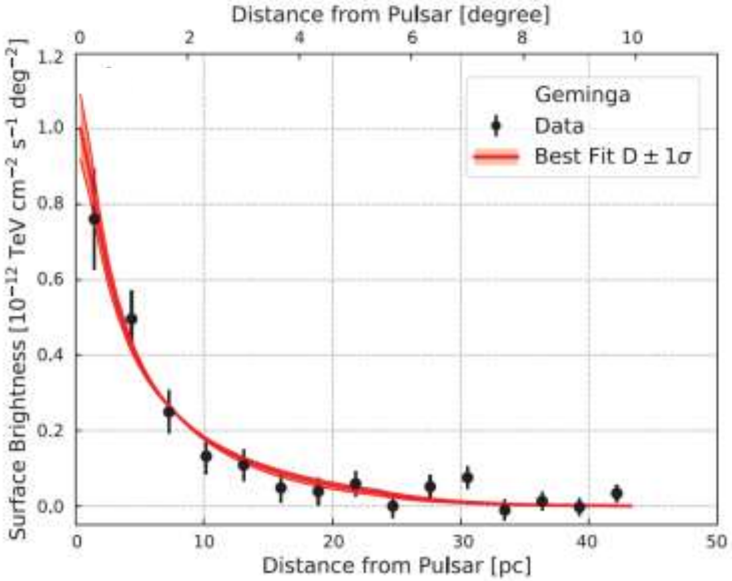

$$\frac{d^2N}{dEd\Omega} = N_0\left(\frac{E}{20\text{TeV}}\right)^{-\alpha}$$

$$\times \frac{1.22}{\pi^{3/2}\theta_d(E)[\theta + 0.06\theta_d(E)]} e^{[-\theta^2/\theta_d(E)^2]}$$

Power-Law spectrum index = 2.34

HWAC Coll. DOI: 10.1126/science.aan4880

Extension and spectrum of PSR B1706-44

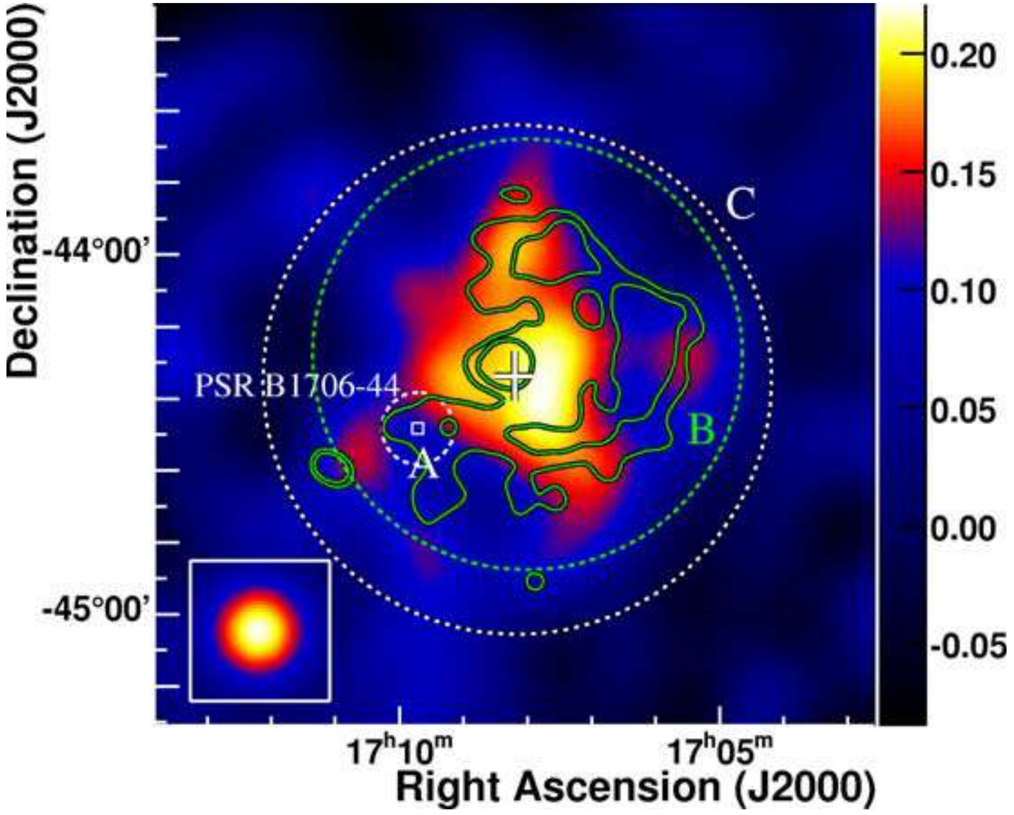

Extension = 0.29 degree

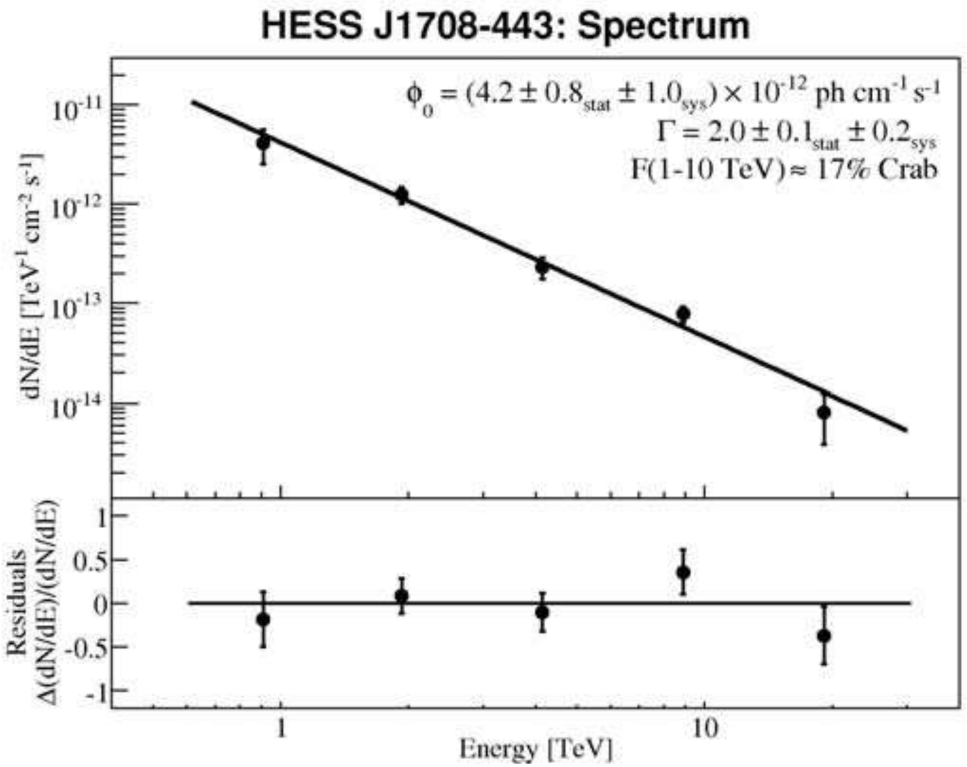

Power-law spectrum index = 2.0

HESS Coll. DOI: 10.1051/0004-6361/201015381

Pulsar	Surrounding PWN	σ (deg)	N_0 ($\mathrm{cm^{-2}s^{-1}TeV^{-1}}$)	E_0 (TeV)	Γ	E_{cut} (TeV)
Crab pulsar	Crab Nebula	0.014	$(8.2 \pm 0.2) \times 10^{-14}$	10	$(2.09 \pm 0.01) + (0.19 \pm 0.02) \log_{10}(E/E_0)$	–
Geminga pulsar	Geminga	1.3	$13.6^{+2.0}_{-1.7} \times 10^{-15}$	20	2.34 ± 0.07	–
Vela pulsar	Vela X	0.51	$(11.6 \pm 0.6) \times 10^{-12}$	1	1.36 ± 0.06	13.9 ± 1.6
PSR B1706-44	G343.1-2.3	0.29	$(4.2 \pm 0.8) \times 10^{-12}$	1	2.0 ± 0.1	–

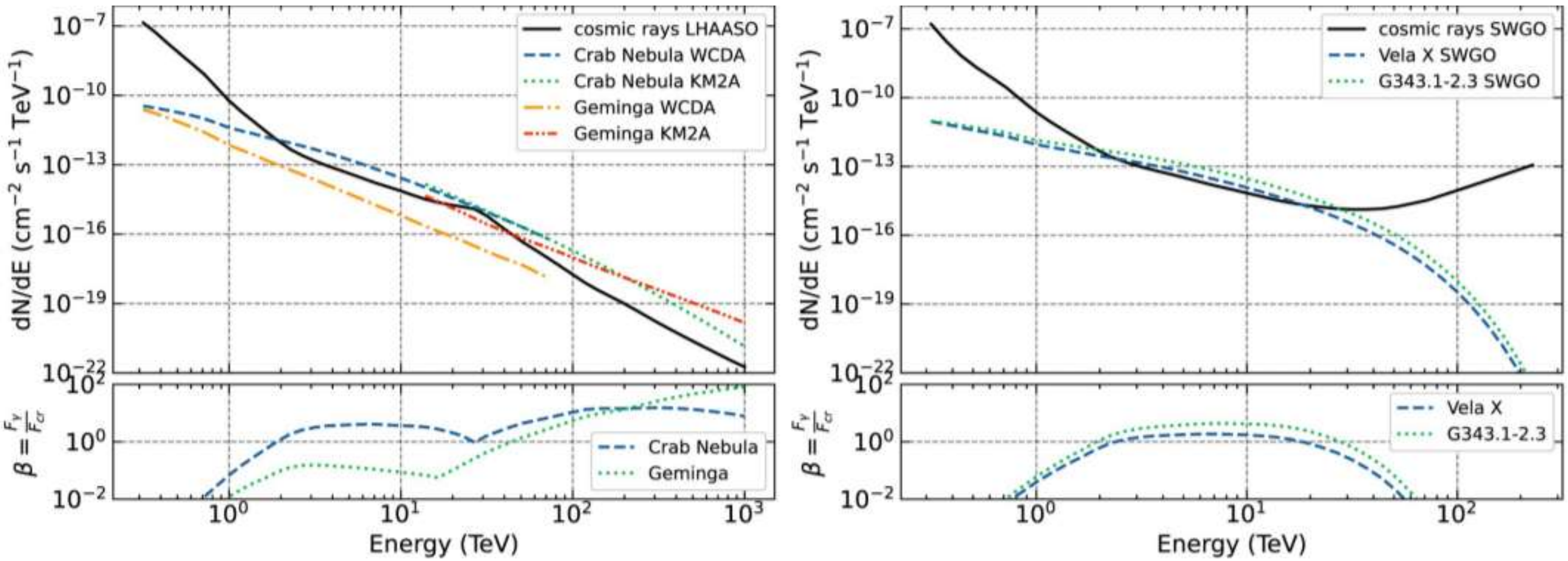

Outline

- Observations of VHE pulsars
- Method for sensitivity of the pulse signal
- Results and summary

Sensitivity of LHAASO and SWGO for pulsar

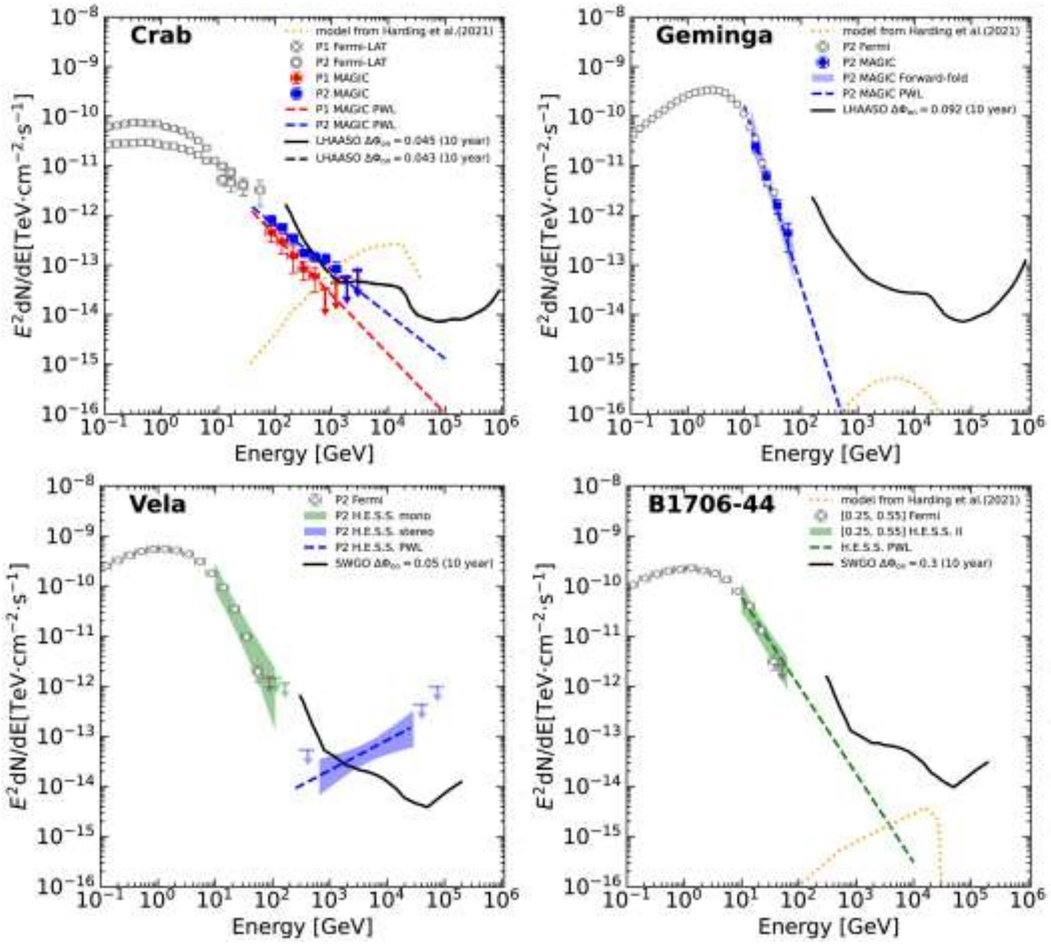

$$F_s^{\mathrm{onP}} = F_s\sqrt{\frac{\alpha(1+\beta)}{n}}$$

Sensitivity for pulsars

Sensitivity for point source

Time(yr)

Expected significance of pulsars

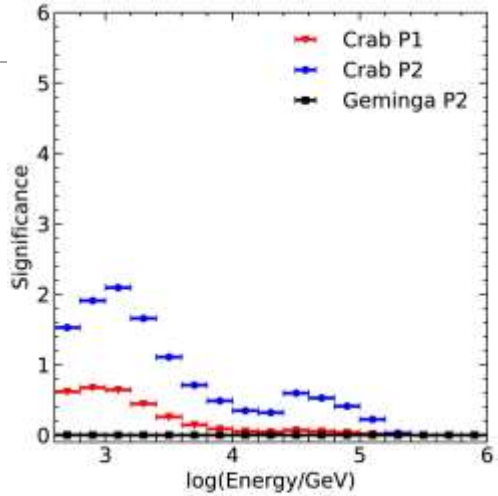

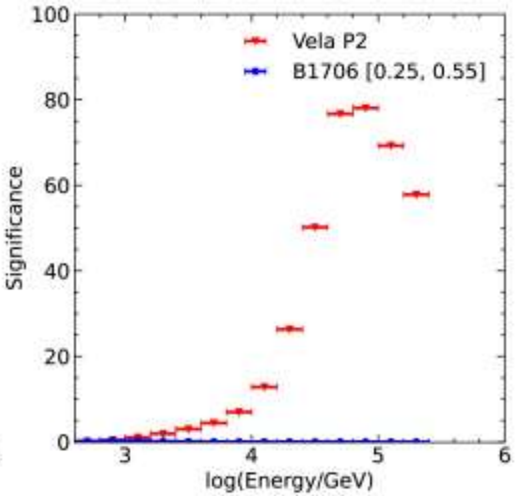

$$S = \frac{5}{\sqrt{\alpha(1+\beta)}} \frac{F^{\mathrm{onP}}}{F_s}$$

Pulsar phase	E_0(GeV)	$N_0(\mathrm{TeV}^{-1}\mathrm{cm}^{-2}\mathrm{s}^{-1})$	Γ	On-pulse fraction	Experiment	Expected time (yr)
Crab P1 [$-$0.017–0.026]	150	$(1.1 \pm 0.3) \times 10^{-11}$	3.2 ± 0.4	0.043	LHAASO	55 at 630 GeV
Crab P2 [0.377–0.422]	150	$(2.0 \pm 0.3) \times 10^{-11}$	2.9 ± 0.2	0.045	LHAASO	6 at 1 TeV
Geminga P2 [0.550–0.642]	32.15	$(2.28 \pm 0.74) \times 10^{-9}$	5.62 ± 0.54	0.092	LHAASO	>1000
Vela P2 [0.55–0.6]	4240	$(1.74 \pm 0.52) \times 10^{-15}$	1.4 ± 0.3	0.05	SWGO	$<$1 at $>$6.3 TeV
B1706-44 [0.25-0.55]	20	$(4.3 \pm 0.9) \times 10^{-8}$	3.76 ± 0.36	0.3	SWGO	287 at 630 GeV

Fraction of the on-pulse interval(α)

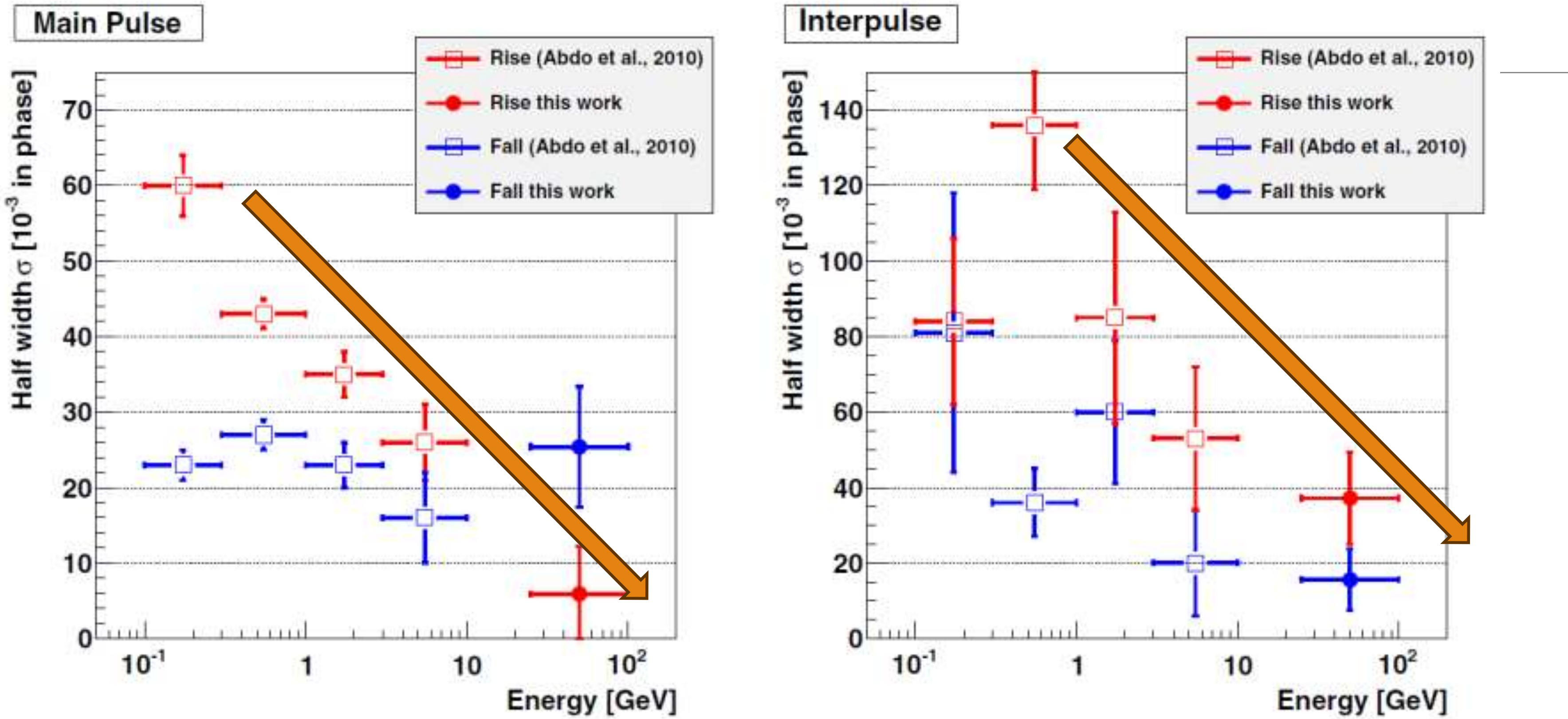

MAGIC Coll. doi:10.1088/0004-637X/742/1/43

The fraction of the on-pulse interval, α, has been shown to decrease with increasing energy. This makes the on-pulse emission from the pulsar more easily detectable in the very-high-energy band.

Summary

- We presented the prospects of detecting four gamma-ray pulsars in the VHE range using LHAASO and SWGO.
- The sensitivity was calculated for the four potential TeV pulsar sources, assuming that the pulsed emission has no HE cutoff and that the energy spectrum can be described by a single power law.
- LHAASO-WCDA is expected to require less than 6 yr to observe the pulsed emission from the Crab pulsar in the VHE range, while Vela's pulsed emission can be observed by SWGO in one year.
- In the absence of an ICS contribution, Crab pulsar are expected to be detectable by LHAASO within a few years. For Geminga pulsar and B1706-44, their predicted flux may be challenging to be observed in 10 yrs.
- LHAASO and SWGO have the advantages of high duty cycles and large field of view, enabling continuous monitoring of pulsars at very-high-energy. Observations of these pulsars at energies above 1 TeV will help us to unravel the mechanism of the TeV component.

Summary

- We presented the prospects of detecting four gamma-ray pulsars in the VHE range using LHAASO and SWGO.
- The sensitivity was calculated for the four potential TeV pulsar sources, assuming that the pulsed emission has no HE cutoff and that the energy spectrum can be described by a single power law.
- LHAASO-WCDA is expected to require less than 6 yr to observe the pulsed emission from the Crab pulsar in the VHE range, while Vela's pulsed emission can be observed by SWGO in one year.
- In the absence of an ICS contribution, Crab pulsar are expected to be detectable by LHAASO within a few years. For Geminga pulsar and B1706-44, their predicted flux may be challenging to be observed in 10 yrs.
- LHAASO and SWGO have the advantages of high duty cycles and large field of view, enabling continuous monitoring of pulsars at very-high-energy. Observations of these pulsars at energies above 1 TeV will help us to unravel the mechanism of the TeV component.

Thanks for your attention!

backup

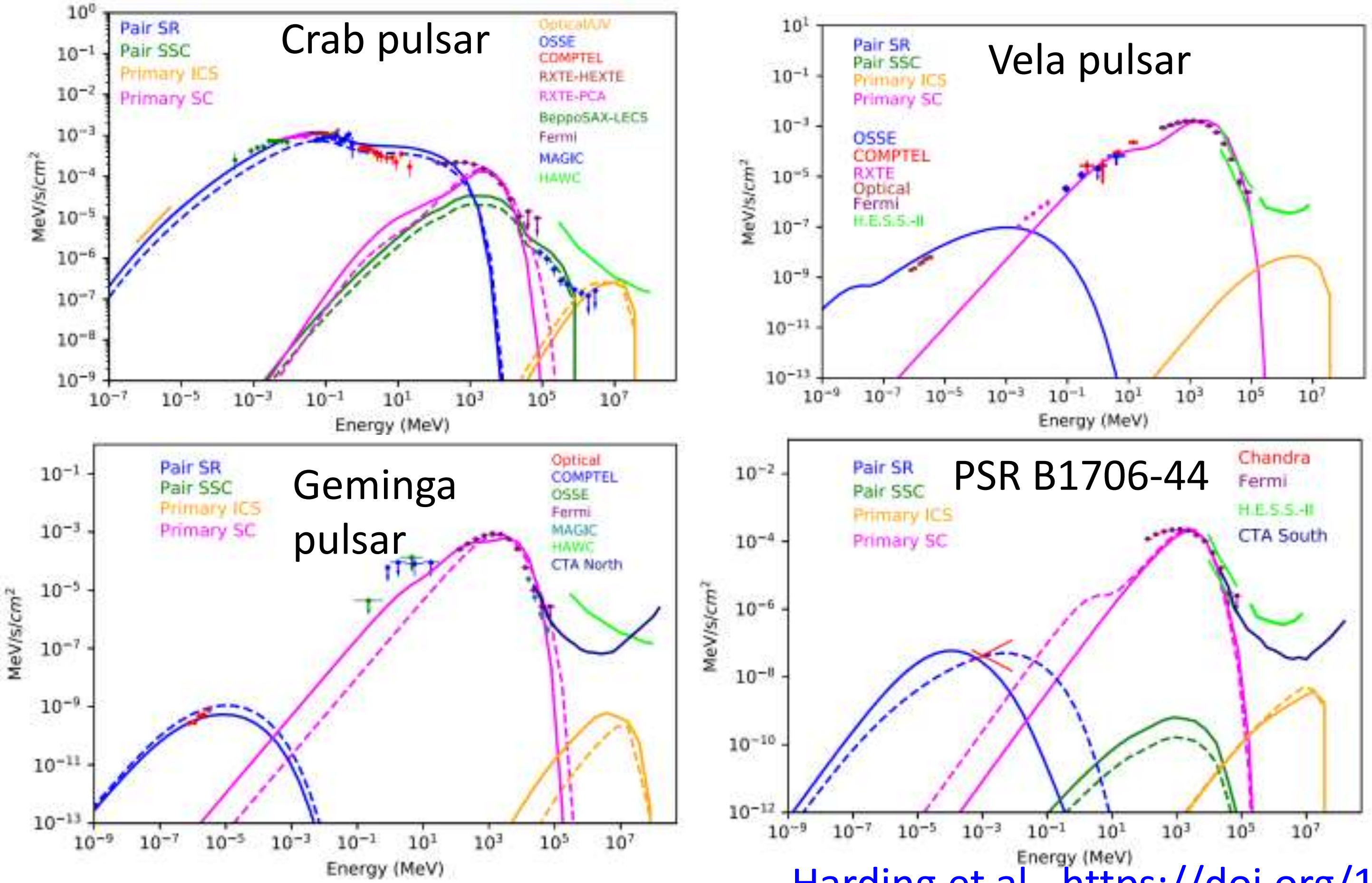

Harding et al., https://doi.org/10.3847/1538-4357/ac3084